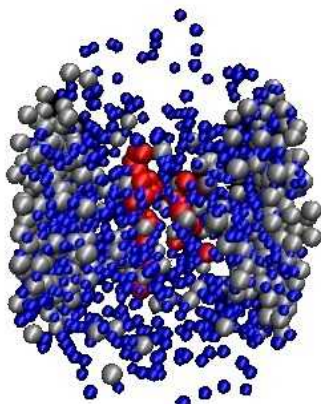




Parton-Hadron Matter at Finite Temperature and Chemical Potential

Elena Bratkovskaya

Institut für Theoretische Physik & FIAS,
Uni. Frankfurt

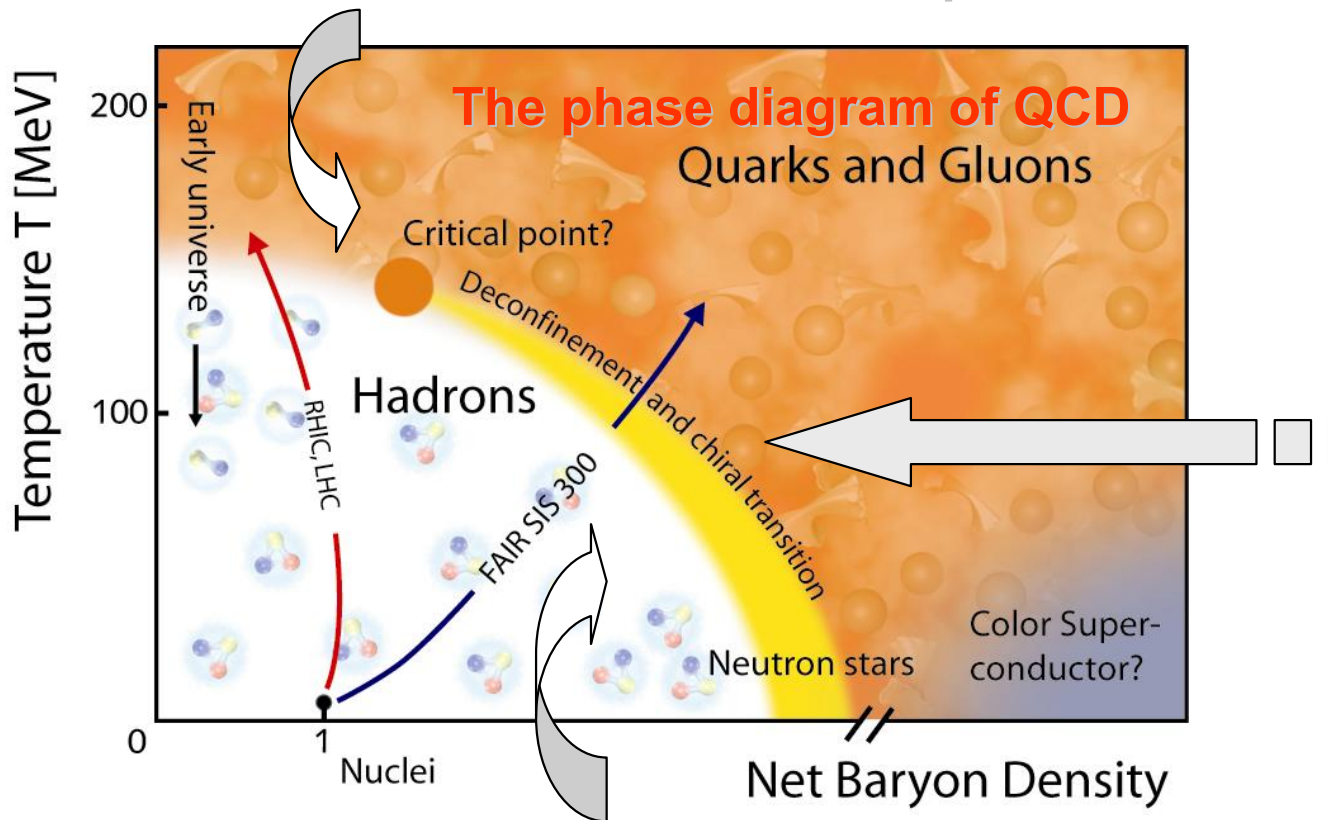


*Keystone, Colorado, USA
25-31 January 2015*



The holy grail of heavy-ion physics:

- Search for the **critical point**



- Study of the **phase transition** from **hadronic** to **partonic** matter – **Quark-Gluon-Plasma**

- Study of the **in-medium** properties of hadrons at high baryon density and temperature

The goal: to **study of the phase transition** from hadronic to partonic matter and properties of the Quark-Gluon-Plasma from **microscopic origin**



Parton-Hadron-String-Dynamics (PHSD)

PHSD is a **non-equilibrium transport model** with

- explicit **phase transition** from hadronic to partonic degrees of freedom
- **IQCD EoS** for the partonic phase (‘crossover’ at $\mu_q=0$)
- explicit **parton-parton interactions** - between quarks and gluons
- **dynamical hadronization**

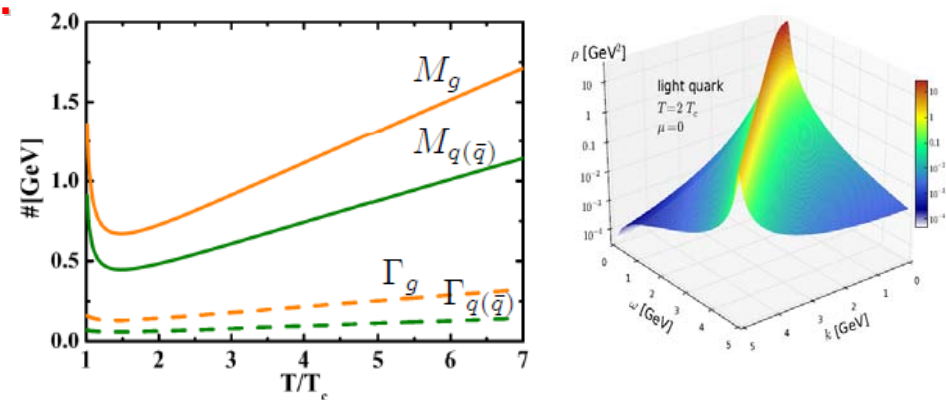
QGP phase is described by the **Dynamical QuasiParticle Model (DQPM) matched to reproduce lattice QCD**

- **strongly interacting quasi-particles:** massive quarks and gluons (g, q, \bar{q}) with sizeable collisional widths in self-generated **mean-field potential**

- **Spectral functions:**

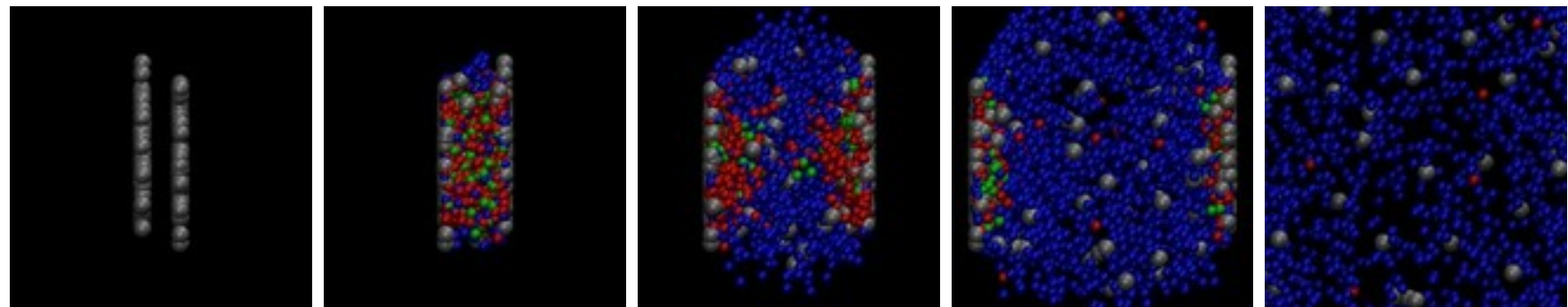
$$\rho_i(\omega, T) = \frac{4\omega\Gamma_i(T)}{\left(\omega^2 - \vec{p}^2 - M_i^2(T)\right)^2 + 4\omega^2\Gamma_i^2(T)}$$

A. Peshier, W. Cassing, PRL 94 (2005) 172301;
W. Cassing, NPA 791 (2007) 365; NPA 793 (2007)



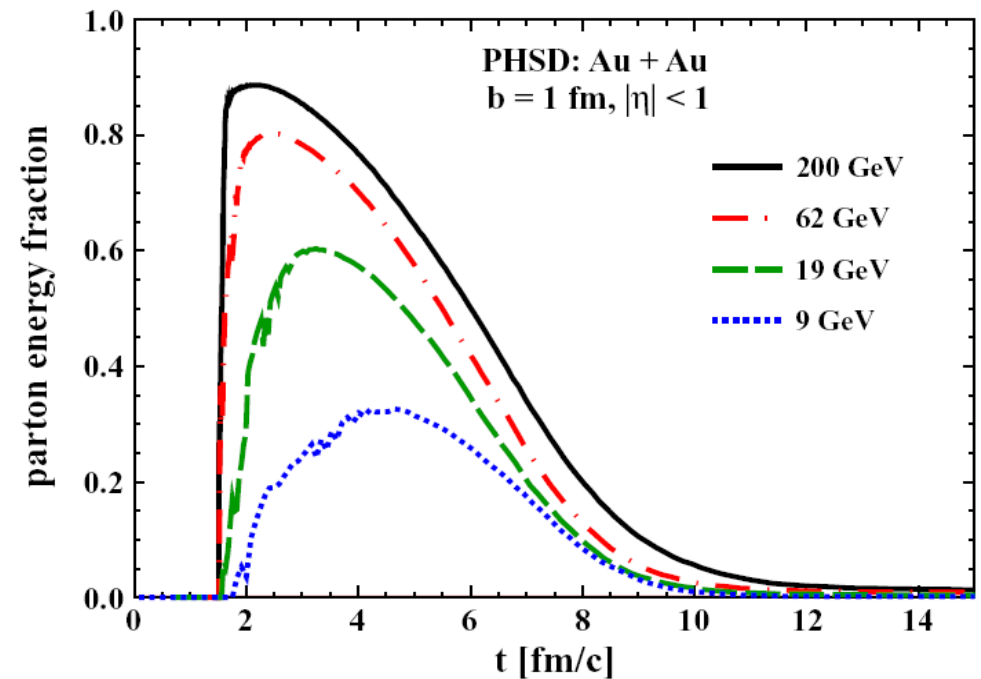
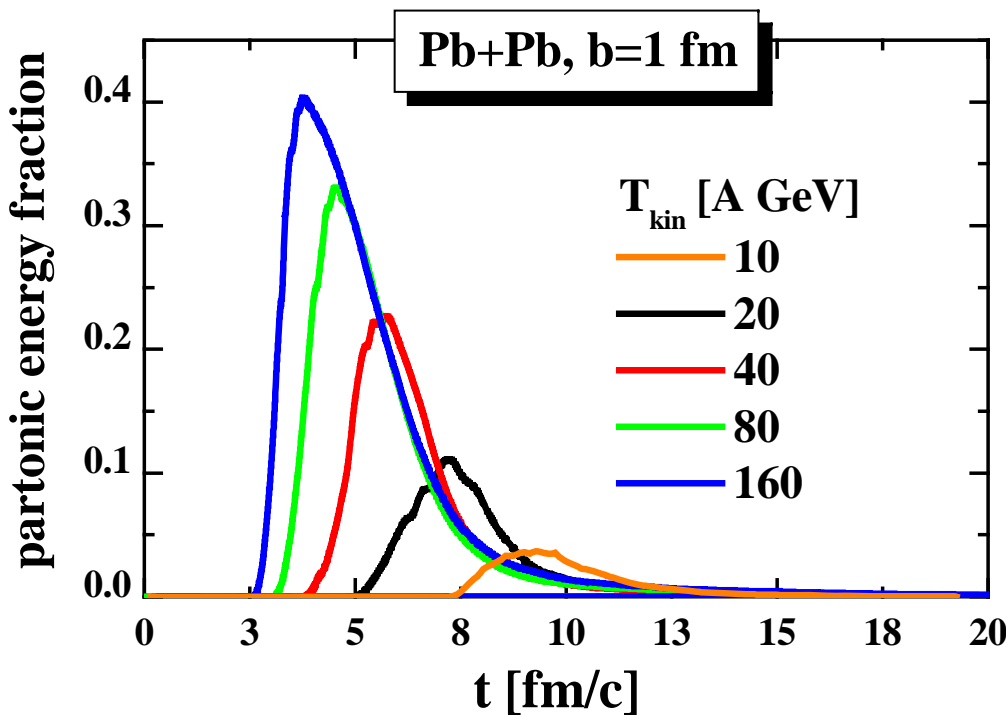
Transport theory: generalized off-shell transport equations based on the 1st order gradient expansion of Kadanoff-Baym equations (**applicable for strongly interacting system!**)

,Bulk' properties in Au+Au collisions

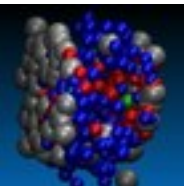


Partonic energy fraction in central A+A

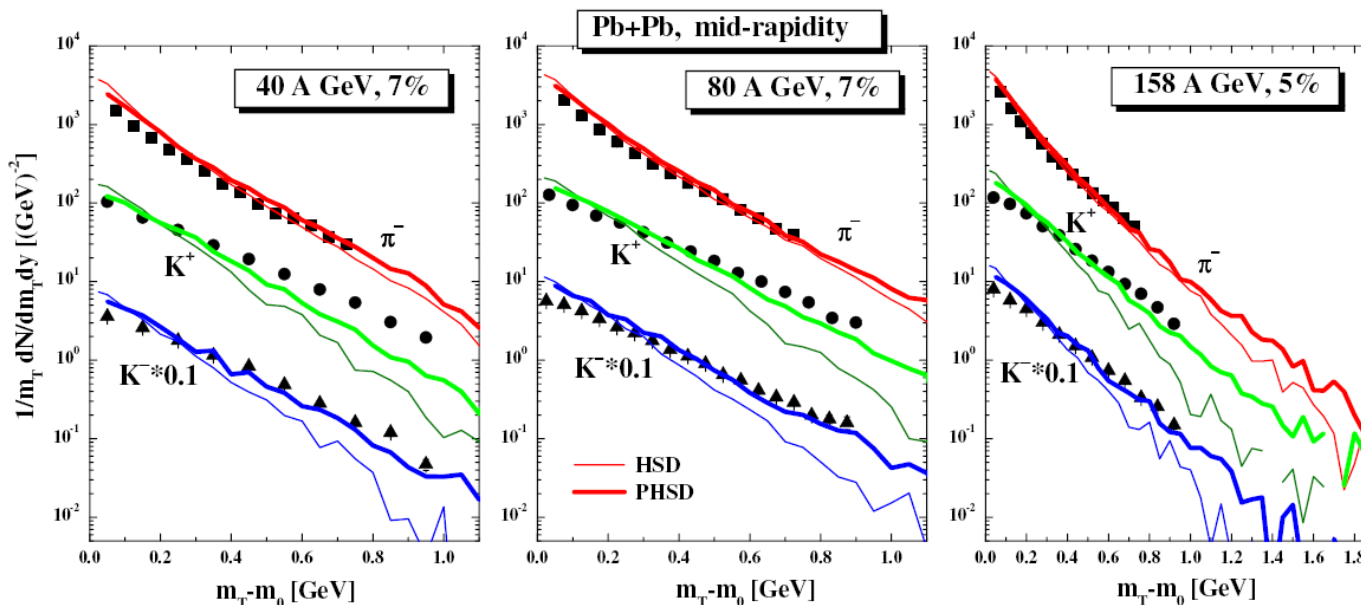
Time evolution of the partonic energy fraction vs energy



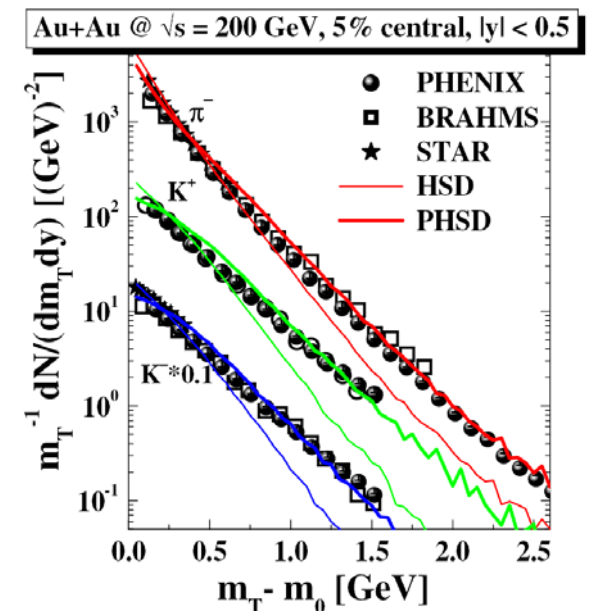
- ❑ Strong increase of partonic phase with energy from AGS to RHIC
- ❑ SPS: Pb+Pb, 160 A GeV: only about 40% of the converted energy goes to partons; the rest is contained in the large hadronic corona and leading partons
- ❑ RHIC: Au+Au, 21.3 A TeV: up to 90% - QGP



Central Pb + Pb at SPS energies



Central Au+Au at RHIC

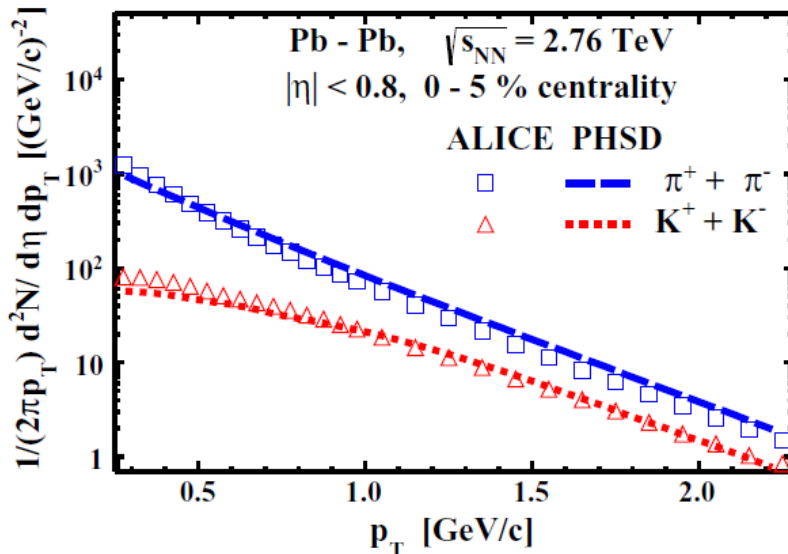


- PHSD gives **harder m_T spectra** and works better than HSD (wo QGP) at high energies – RHIC, SPS (and top FAIR, NICA)
- however, at **low SPS** (and low FAIR, NICA) energies the **effect of the partonic phase decreases** due to the decrease of the partonic fraction

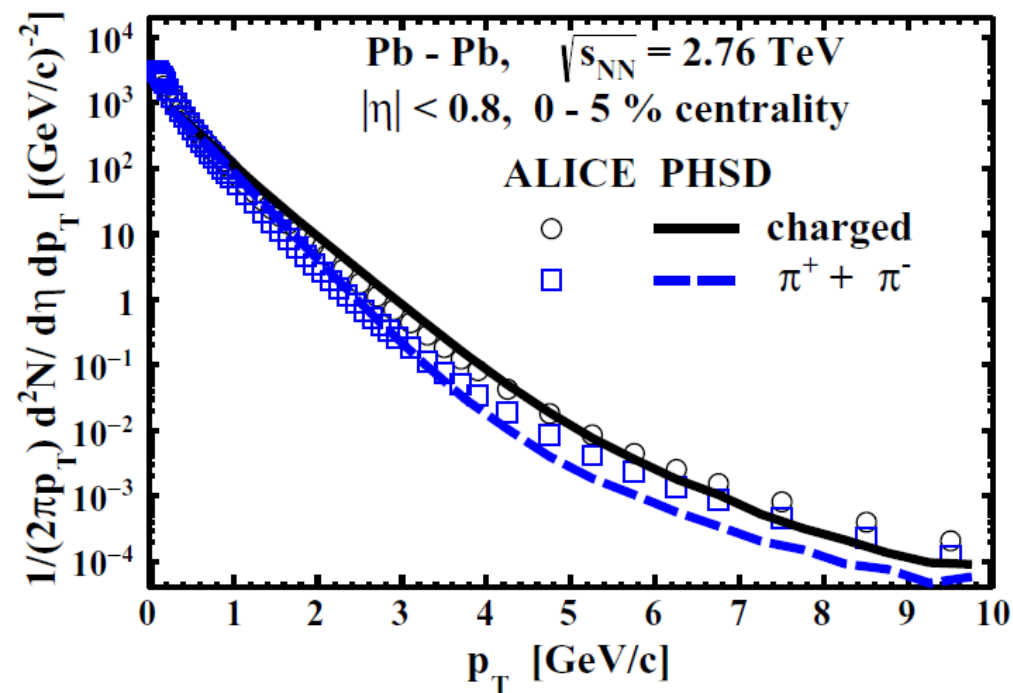
W. Cassing & E. Bratkovskaya, NPA 831 (2009) 215
 E. Bratkovskaya, W. Cassing, V. Konchakovski,
 O. Linnyk, NPA856 (2011) 162

p_T spectra for Pb+Pb from PHSD at LHC

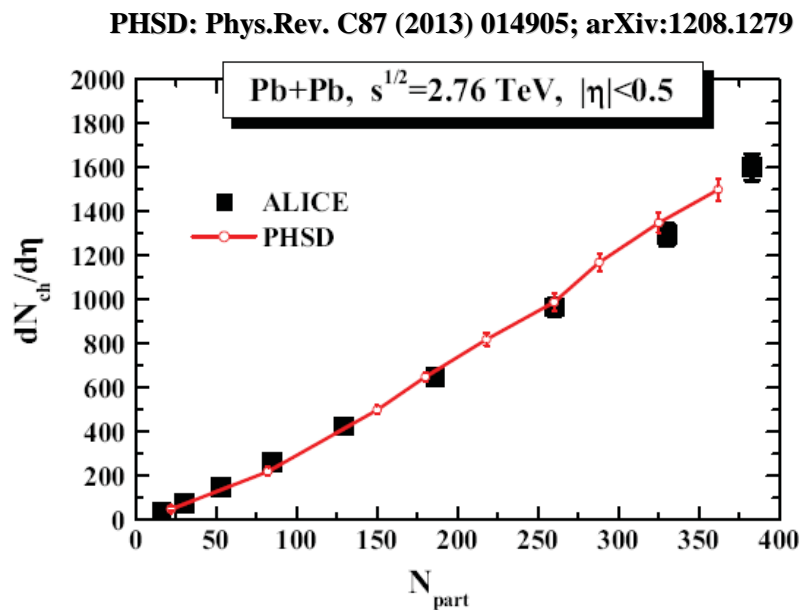
Low p_T spectra of pions and kaons



p_T spectra of charged hadrons and pions central Pb+Pb at $s^{1/2}=2.76$ TeV



Charged particle multiplicity vs centrality

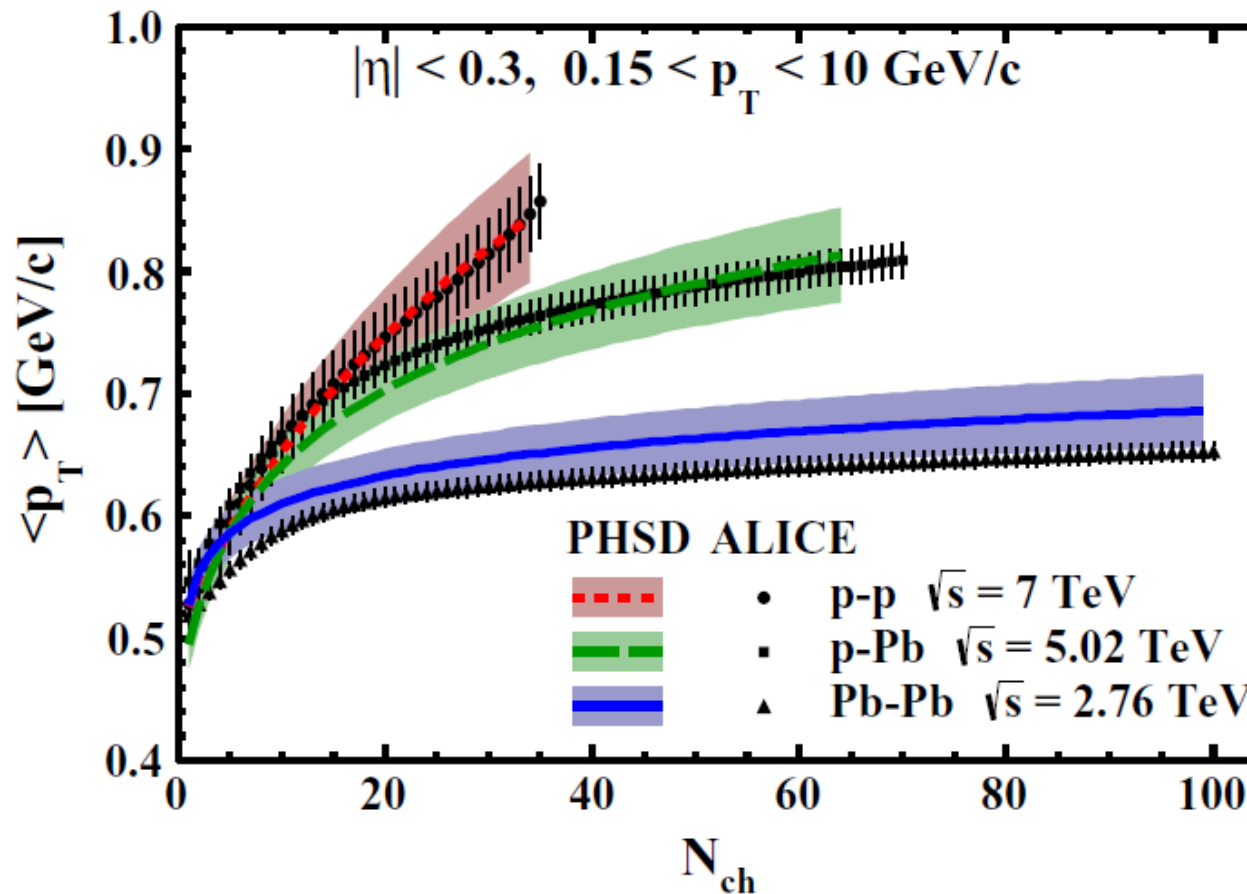


→ PHSD reproduces ALICE data on Pb+Pb

V. Konchakovski, W. Cassing, V. Toneev, arXiv:1411.5534

Correlations of mean p_T vs N_{ch} at LHC

Mean p_T of charged hadrons at midrapidity vs N_{ch} for

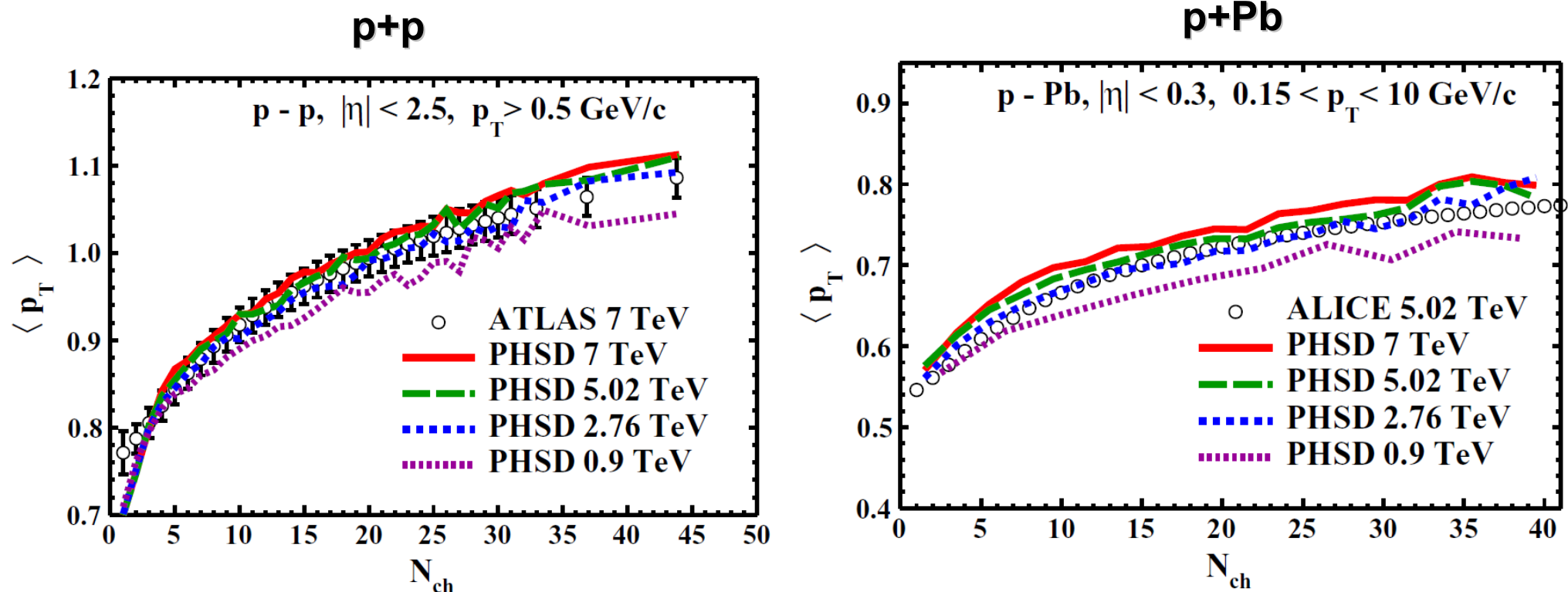


$p+p$ at $s^{1/2}=7$ TeV
 $p+Pb$ at $s^{1/2}=5.02$ TeV,
 $Pb+Pb$ at $s^{1/2}=2.76$ TeV

→ PHSD reproduces
ALICE data on mean p_T

- Why the mean p_T spectra of $p+p$ and $p+Pb$ are identical at low N_{ch} ?
- What is the origin for the ‚hierarchy‘ of mean p_T at larger N_{ch} ?

Energy dependence of mean p_T vs N_{ch} at LHC

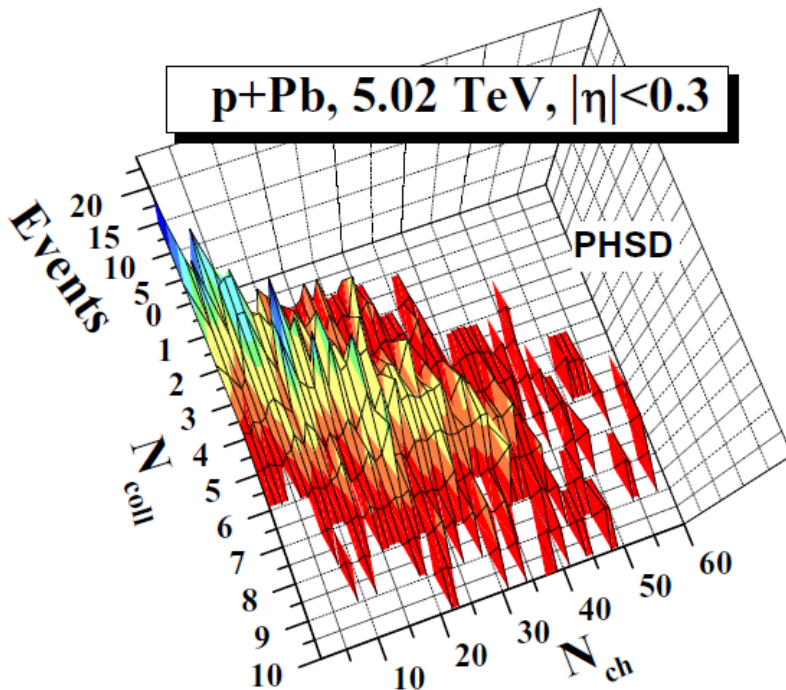


- The correlations of $\langle p_T \rangle$ of charged hadrons at midrapidity vs N_{ch} do not change much at LHC energies from 2.76 to 7 TeV for pp and p+Pb

→ Relatively weak energy dependence of $\langle p_T \rangle$ vs N_{ch}

N_{coll} and N_{ch} correlations in p+Pb at LHC from PHSD

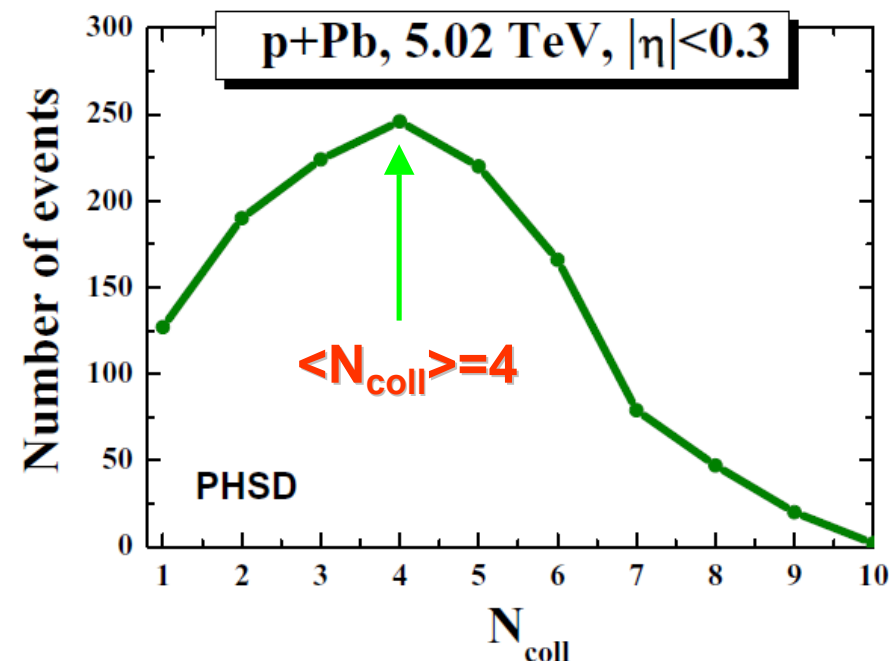
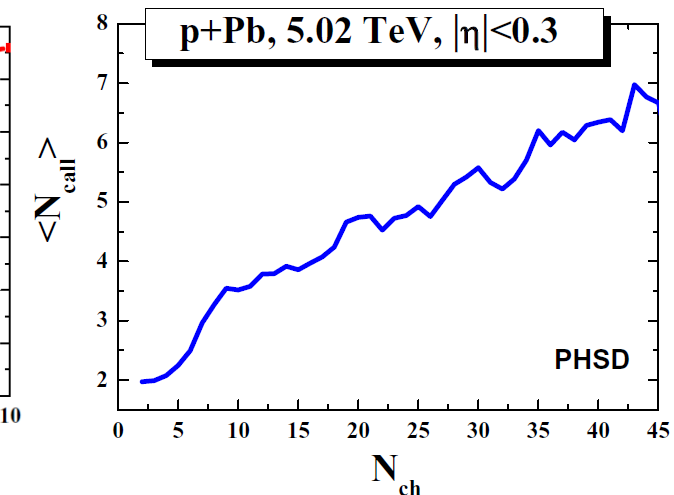
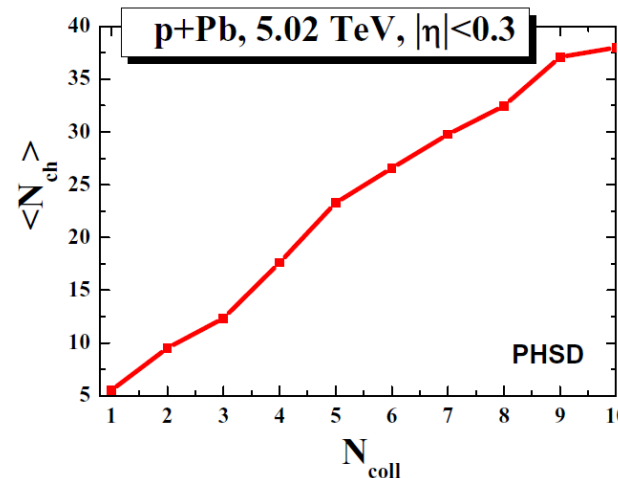
Number of events in p+Pb,
 $|\eta| < 0.3$ vs N_{ch} and N_{coll}



PHSD for p+Pb, $|\eta| < 0.3$:

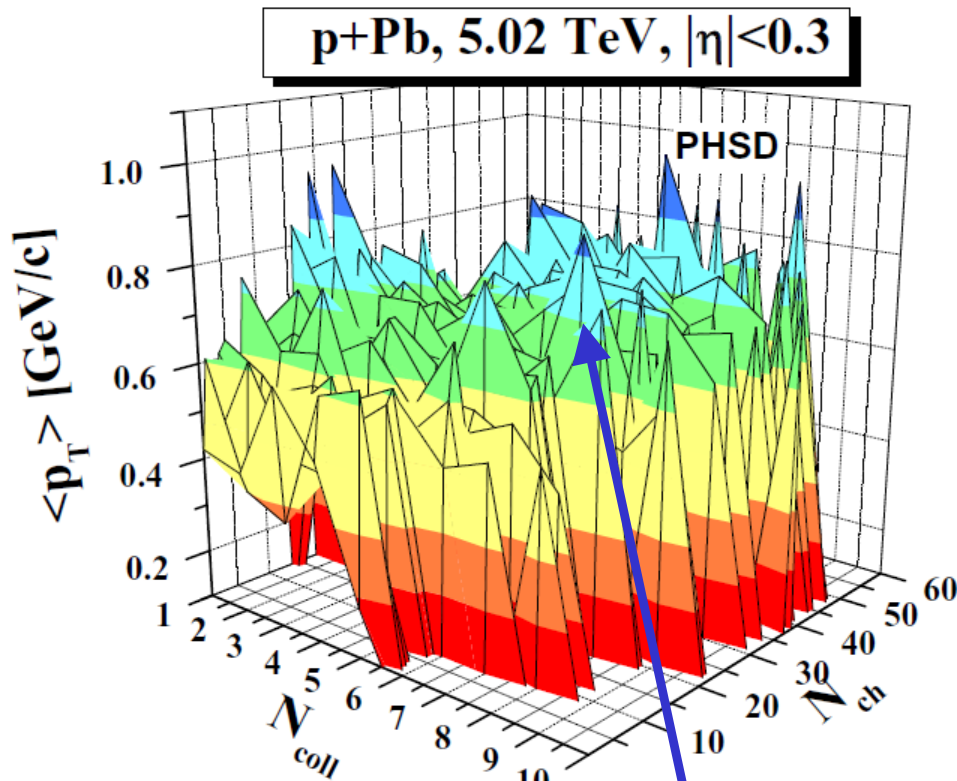
- wide distribution in (N_{coll} , N_{ch});
- no strong correlations between N_{ch} and N_{coll} except for low N_{coll}
- linear dependence of mean values N_{ch} and N_{coll}
- $\langle N_{\text{coll}} \rangle = 4$

Correlations of ,mean values ' N_{ch} and N_{coll}

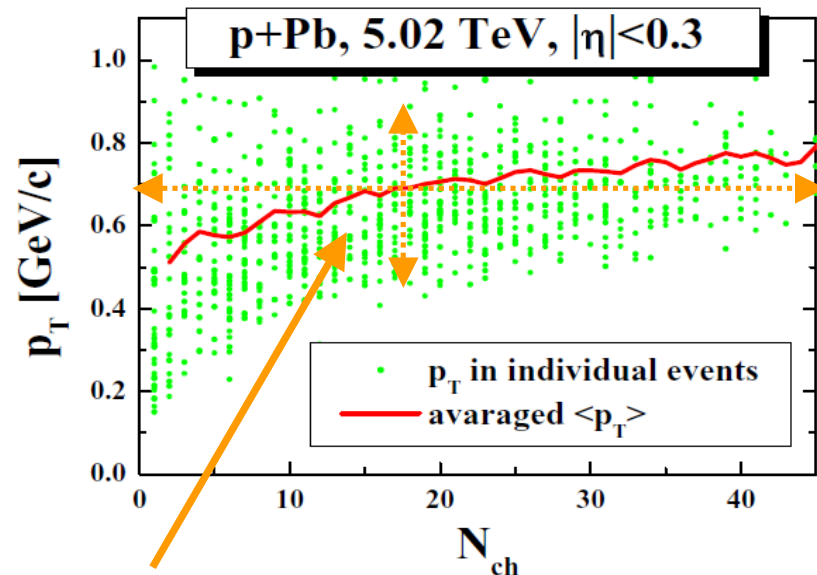


Correlations of p_T vs N_{coll} and N_{ch} in p+Pb from PHSD

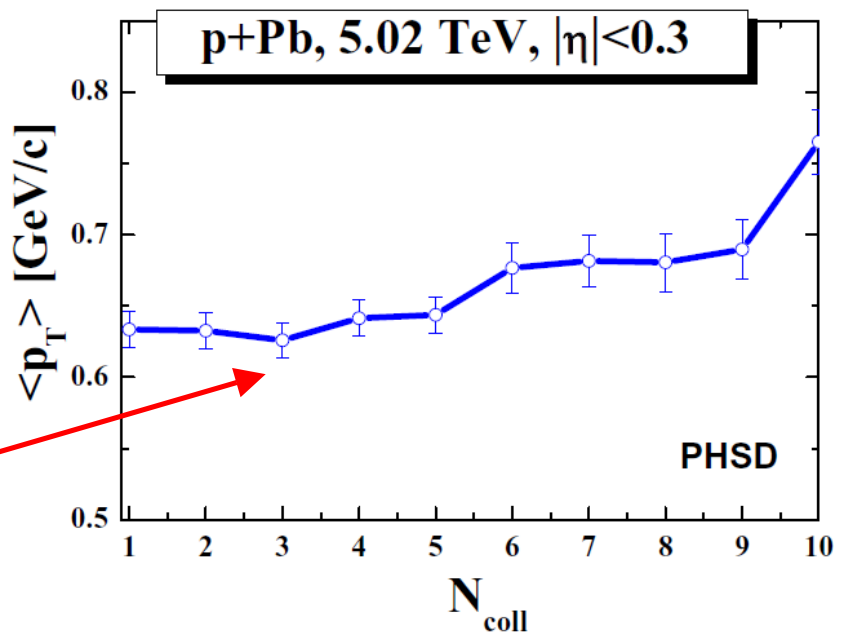
$\langle p_T \rangle$ in p+Pb, $|\eta| < 0.3$
vs. N_{ch} and N_{coll}



→ $\langle p_T \rangle$ is flat vs. (N_{coll} , N_{ch})



→ Huge e-by-e p_T fluctuations vs N_{ch}



Correlations of $\langle p_T \rangle$ vs N_{ch} at LHC



Note!

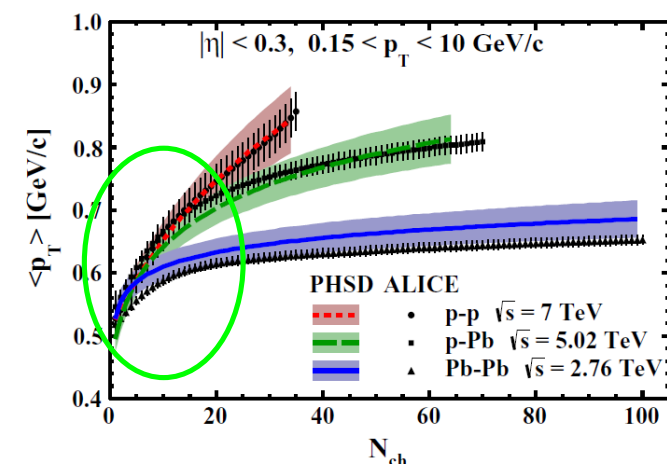
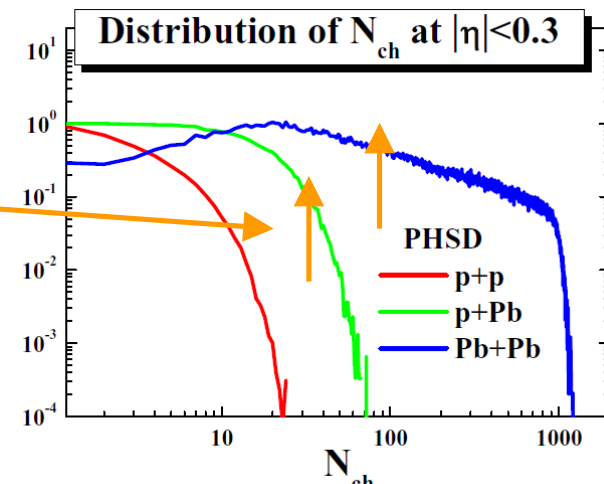
- * probe only narrow part of the total phase space for $|\eta| < 0.3 \rightarrow$ large influence of correlations!
- * probe only peripheral Pb+Pb and up to semi-central p+Pb

The origin for the 'hierarchy' of $\langle p_T \rangle$ vs N_{ch} :

- p+p:** $N_{coll} = 1$; $\langle p_T \rangle$ grows ~linearly with vs. N_{ch}
- p+Pb:** at low $N_{ch} \rightarrow N_{coll} \sim 1-2 \rightarrow$ similar to pp
at larger $N_{ch} \rightarrow N_{coll} \gg 1$
= summation of multiple (soft) collisions !

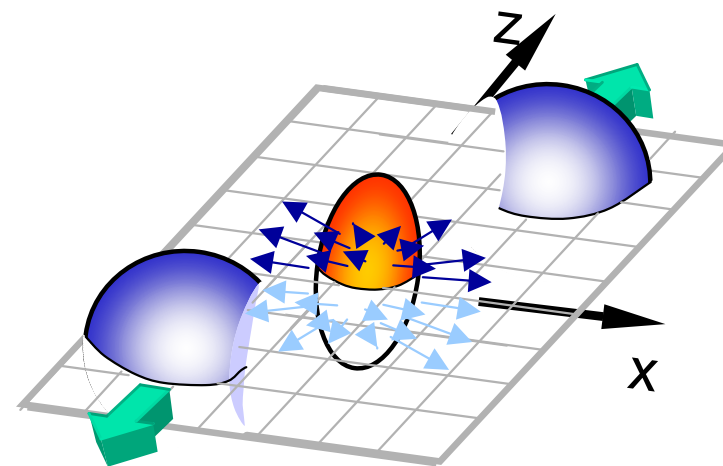
e.g. $\langle N_{coll} \rangle = 4$ corresponds to total $N_{ch} \sim 20$
 \rightarrow in each individual j-collision $N_{ch}(j)$ is small and $p_T(j)$ is small to end up with total $N_{ch} \sim 20$ and $\langle p_T \rangle \sim 0.65 \text{ GeV}/c$

- Pb+Pb:** (similar to p+Pb) – multiple collisions!
! secondary collisions lowering $\langle p_T \rangle$



→ correlations between averages!

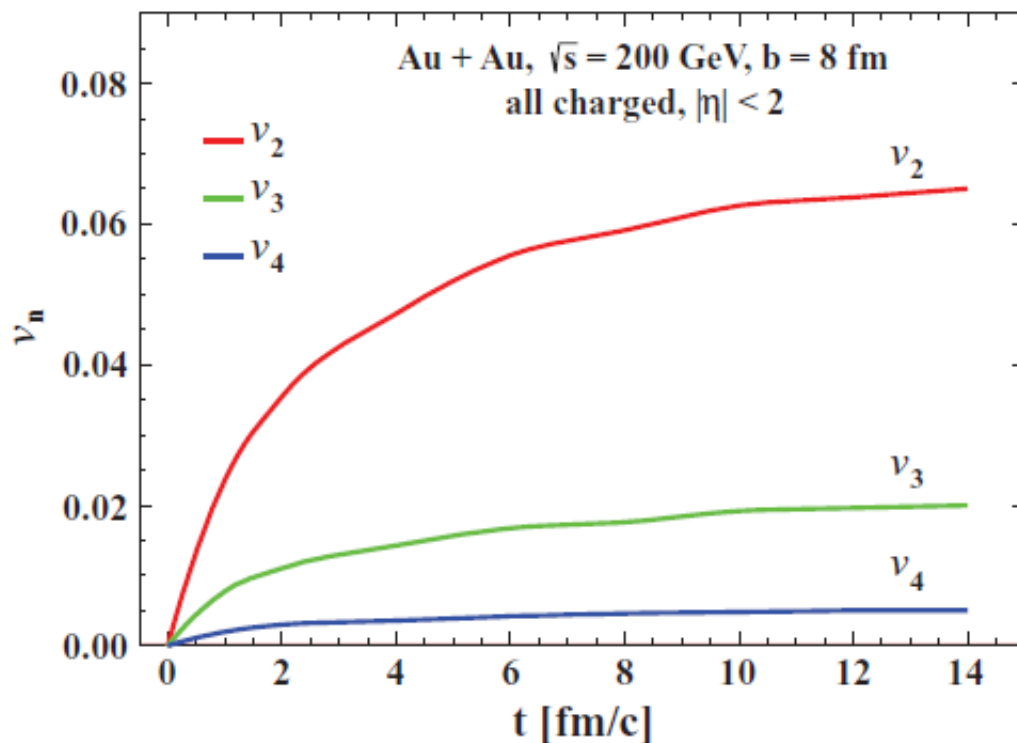
Collective flow, anisotropy coefficients (v_1, v_2, \dots) in A+A



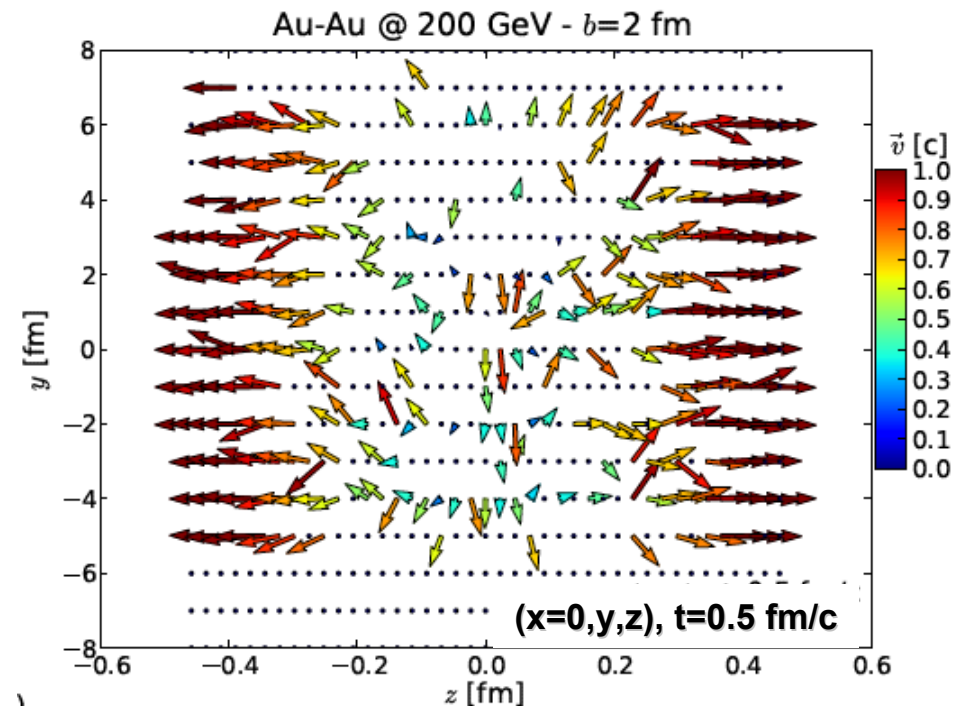
Development of azimuthal anisotropies in time

Au + Au collisions at $s^{1/2} = 200 \text{ GeV}$

□ Time evolution of v_n for $b = 8 \text{ fm}$

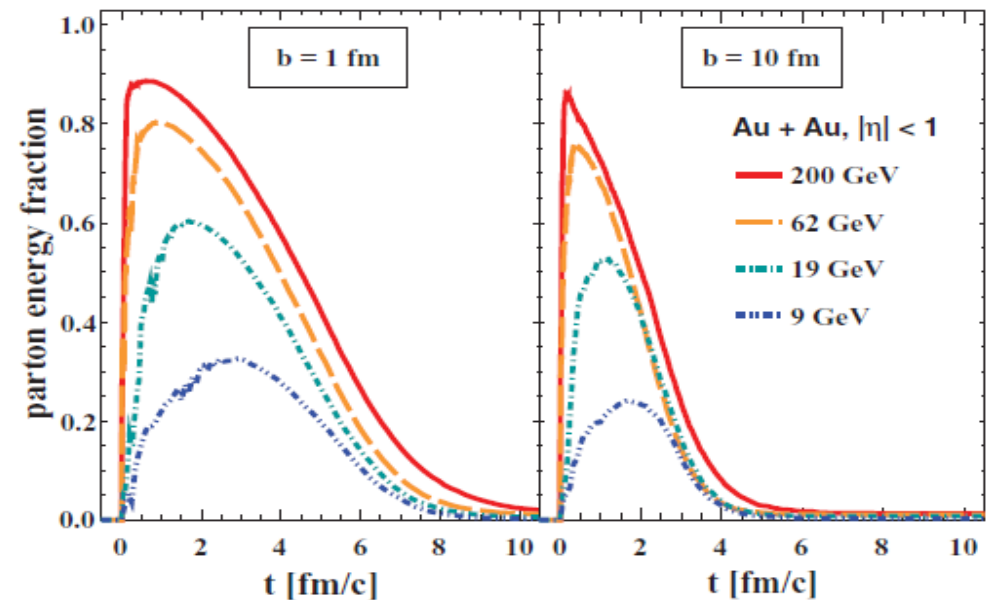
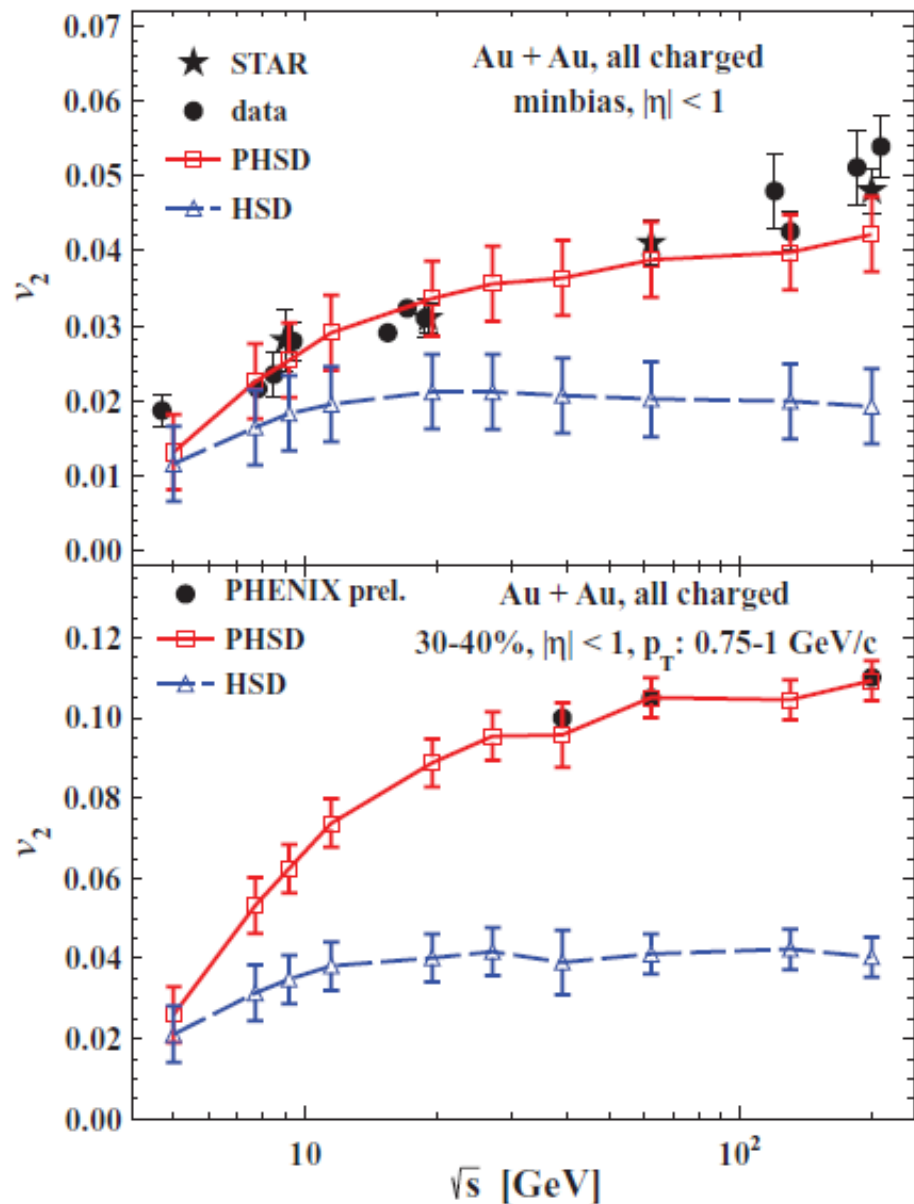


□ Flow velocity for $b = 2 \text{ fm}$
($x=0, y, z$), $t=0.5 \text{ fm/c}$



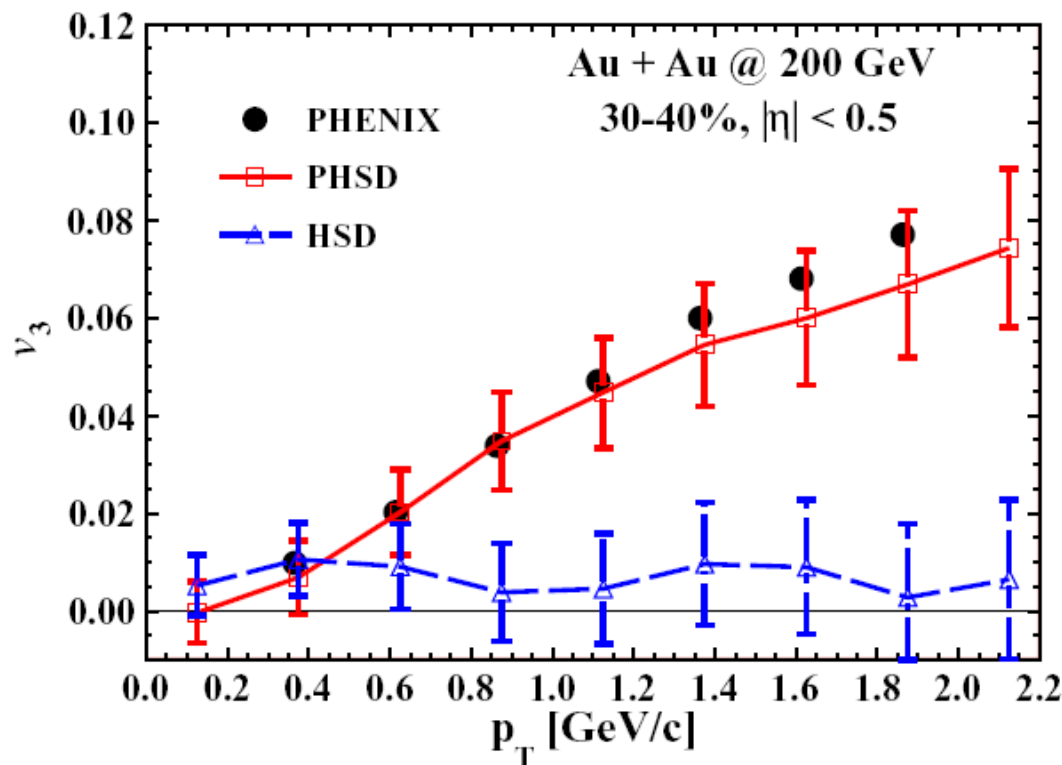
- Flow coefficients reach their asymptotic values by the time of 6–8 fm/c after the beginning of the collision

Elliptic flow v_2 vs. collision energy for Au+Au

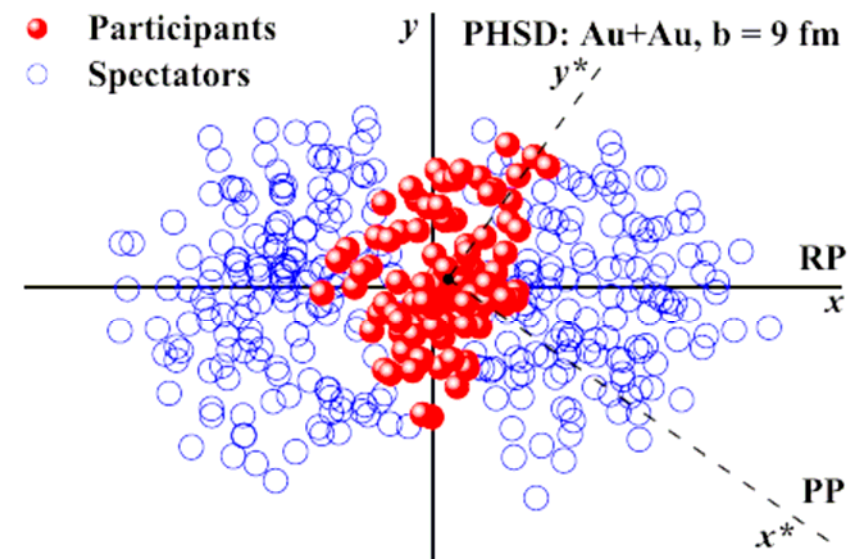


- v_2 in PHSD is larger than in HSD due to the repulsive scalar mean-field potential $U_s(p)$ for partons
- v_2 grows with bombarding energy due to the increase of the parton fraction

Transverse momentum dependence of triangular flow at RHIC

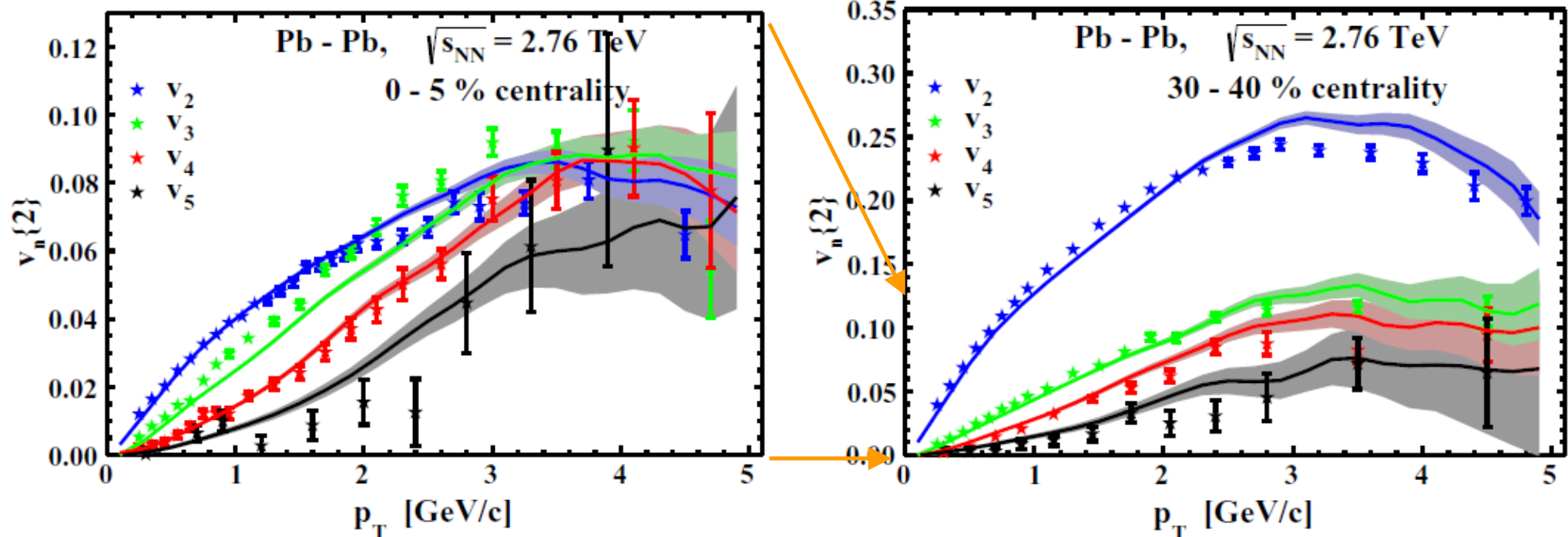


triangular flow



- HSD (without QGP) shows a flat p_T distribution
- PHSD shows an increase of v_3 with p_T
- ➔ v_3 : needs partonic degrees of freedom !

V_n ($n=2,3,4,5$) of charged particles from PHSD at LHC



- PHSD: increase of v_n ($n=2,3,4,5$) with p_T
- v_2 increases with decreasing centrality
- v_n ($n=3,4,5$) show weak centrality dependence

symbols – ALICE

PRL 107 (2011) 032301

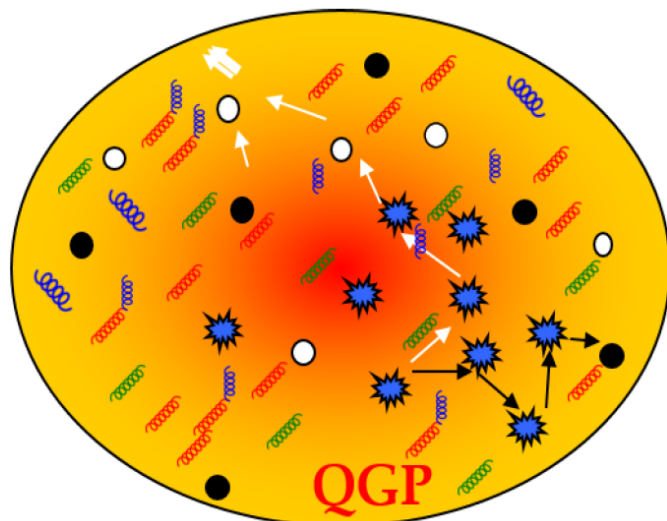
lines – PHSD (e-by-e)



Messages from the study of spectra and collective flow

- PHSD gives harder m_T spectra than HSD (without QGP) at high energies – LHC, RHIC, SPS
- at RHIC and LHC the QGP dominates the early stage dynamics
- at low SPS (and low FAIR, NICA) energies the effect of the partonic phase decreases
 - influence of the finite quark chemical potential μ_q ?!
- Anisotropy coefficients v_n as a signal of the QGP:
 - quark number scaling of v_2 at ultrarelativistic energies – signal of deconfinement
 - growing of v_2 with energy – partonic interactions generate a larger pressure than the hadronic interactions
 - v_n , $n=3,..$ – sensitive to QGP

Thermodynamic and transport properties of sQGP in equilibrium at finite temperature and chemical potential



Hamza Berrehrah et al.

The Dynamical QuasiParticle Model (DQPM) at finite T

Properties of interacting quasi-particles:
massive quarks and gluons (g, q, \bar{q} , q_{bar})
with Lorentzian spectral functions:

$$A_i(\omega, T) = \frac{4\omega\Gamma_i(T)}{\left(\omega^2 - \vec{p}^2 - M_i^2(T)\right)^2 + 4\omega^2\Gamma_i^2(T)}$$

$(i = q, \bar{q}, g)$

■ Modeling of the quark/gluon masses and widths → HTL limit at high T

■ quarks:

mass: $M_{q(\bar{q})}^2(T) = \frac{N_c^2 - 1}{8N_c} g^2 \left(T^2 + \frac{\mu_q^2}{\pi^2} \right)$

width: $\Gamma_{q(\bar{q})}(T) = \frac{1}{3} \frac{N_c^2 - 1}{2N_c} \frac{g^2 T}{8\pi} \ln\left(\frac{2c}{g^2} + 1\right)$

■ gluons:

$$M_g^2(T) = \frac{g^2}{6} \left(\left(N_c + \frac{N_f}{2} \right) T^2 + \frac{N_c}{2} \sum_q \frac{\mu_q^2}{\pi^2} \right)$$

$$\Gamma_g(T) = \frac{1}{3} N_c \frac{g^2 T}{8\pi} \ln\left(\frac{2c}{g^2} + 1\right)$$

$N_c = 3, N_f = 3$

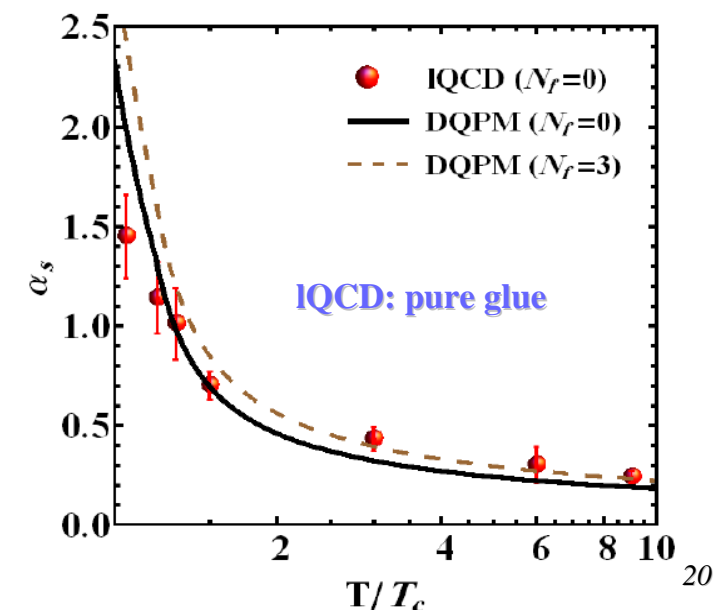
■ running coupling (pure glue):

$$\alpha_s(T) = \frac{g^2(T)}{4\pi} = \frac{12\pi}{(11N_c - 2N_f) \ln[\lambda^2(T/T_c - T_s/T_c)^2]}$$

□ fit to lattice (IQCD) results (e.g. entropy density)

with 3 parameters: $T_s/T_c = 0.46$; $c = 28.8$; $\lambda = 2.42$
 (for pure glue $N_f = 0$)

DQPM: Peshier, Cassing, PRL 94 (2005) 172301;
 Cassing, NPA 791 (2007) 365; NPA 793 (2007)



DQPM at finite (T, μ_q) : scaling hypothesis

- Scaling hypothesis for the effective temperature T^* for $N_f = N_c = 3$

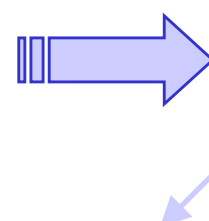
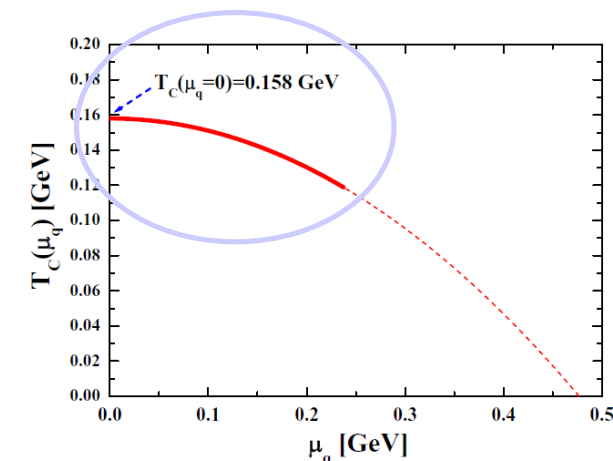
$$T^{*2} = T^2 + \frac{\mu_q^2}{\pi^2}$$

$$\mu_u = \mu_d = \mu_s = \mu_q$$

- Coupling constant:

$$g(T/T_c(\mu = 0)) \rightarrow g(T^*/T_c(\mu))$$

- Critical temperature $T_c(\mu_q)$: obtained by requiring a constant energy density ε for the system at $T = T_c(\mu_q)$ where ε at $T_c(\mu_q=0)=158$ GeV is fixed by IQCD at $\mu_q=0$



$$\frac{T_c(\mu_q)}{T_c(\mu_q = 0)} = \sqrt{1 - \alpha \mu_q^2} \approx 1 - \alpha/2 \mu_q^2 + \dots$$

$$\alpha \approx 8.79 \text{ GeV}^{-2}$$

- ! Consistent with lattice QCD:

IQCD: C. Bonati et al., PRC90 (2014) 114025

$$\frac{T_c(\mu_B)}{T_c} = 1 - \kappa \left(\frac{\mu_B}{T_c} \right)^2 + \dots$$

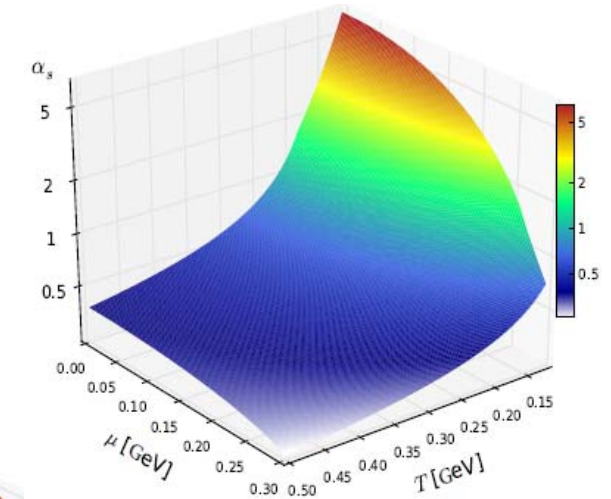
$$\text{IQCD } \kappa = 0.013(2) \quad \longleftrightarrow \quad \kappa_{DQPM} \approx 0.0122$$

H. Berrehrah et al. arXiv:1412.1017

DQPM at finite (T, μ_q) : quasiparticle masses and widths

□ Coupling constant:

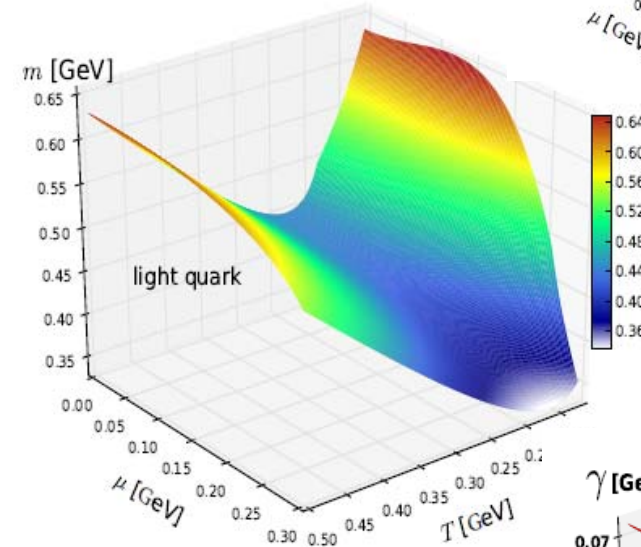
$$g^2(T^*/T_c(\mu_q)) = \frac{48\pi^2}{(11N_c - 2N_f) \ln \left(\lambda^2 \left(\frac{T^*}{T_c(\mu_q)} - \frac{T_s}{T_c(\mu_q)} \right)^2 \right)}$$



□ Quark and gluon masses:

$$M_g^2(T^*, \mu_q) = \frac{g^2(T^*/T_c(\mu_q))}{6} \left(N_c + \frac{1}{2} N_f \right) T^{*2},$$

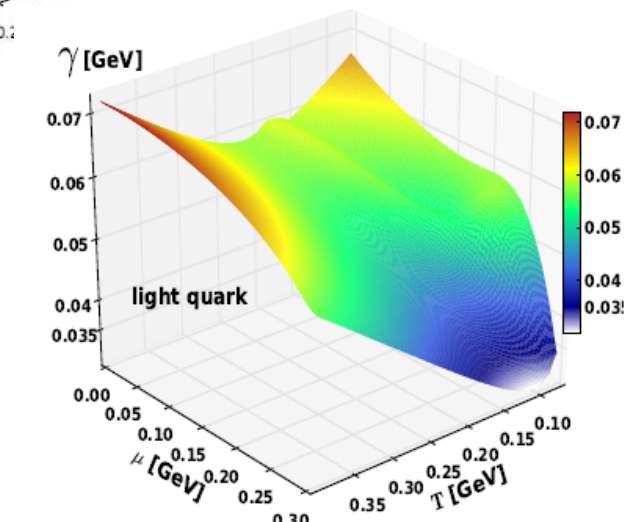
$$M_q^2(T^*, \mu_q) = \frac{N_c^2 - 1}{8N_c} g^2(T^*/T_c(\mu_q)) T^{*2},$$



□ Quark and gluon widths:

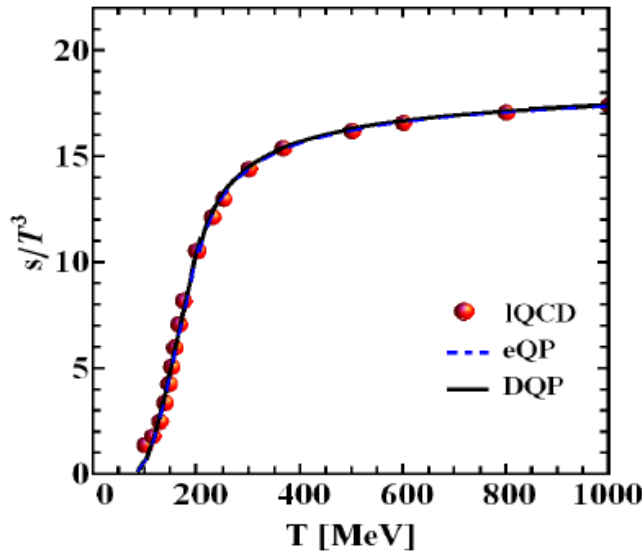
$$\gamma_g(T, \mu_q) = \frac{1}{3} N_c \frac{g^2(T^*/T_c(\mu_q))}{8\pi} T \ln \left(\frac{2c}{g^2(T^*/T_c(\mu_q))} + 1 \right),$$

$$\gamma_q(T, \mu_q) = \frac{1}{3} \frac{N_c^2 - 1}{2N_c} \frac{g^2(T^*/T_c(\mu_q))}{8\pi} T \ln \left(\frac{2c}{g^2(T^*/T_c(\mu_q))} + 1 \right).$$

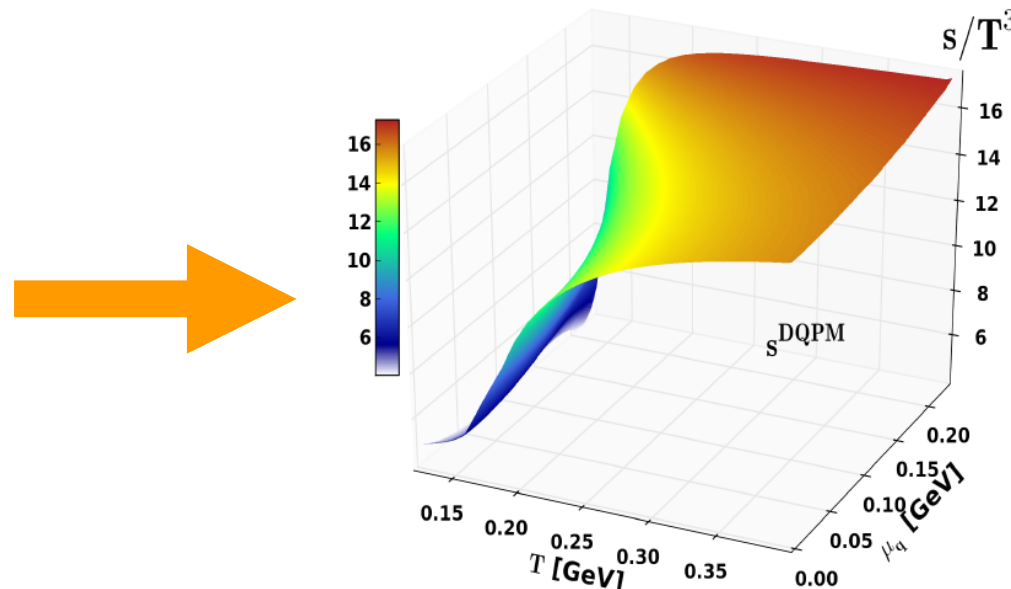


DQPM: thermodynamics at finite (T, μ_q)

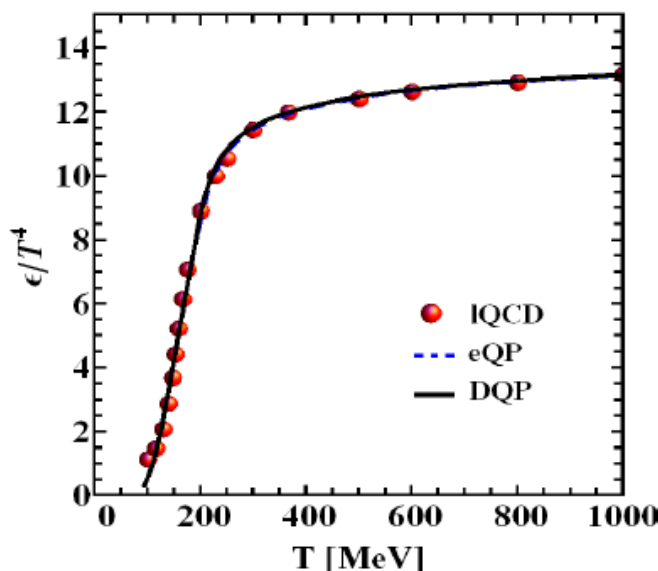
□ Entropy density at finite T



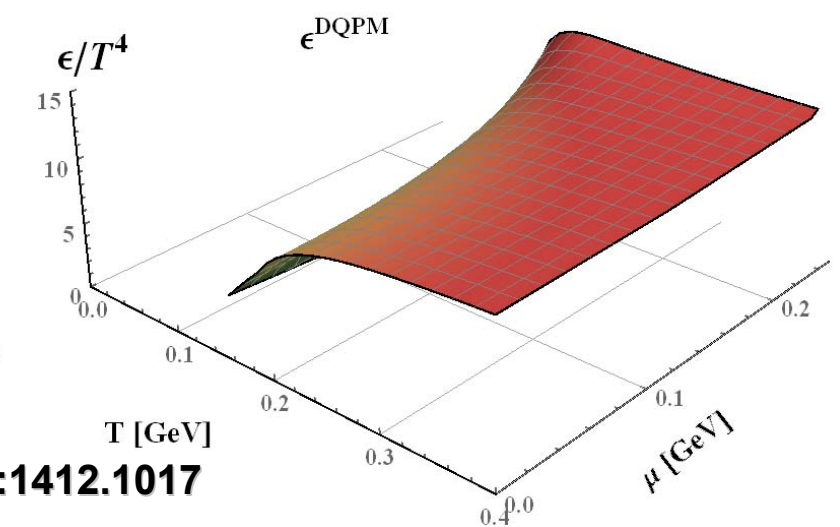
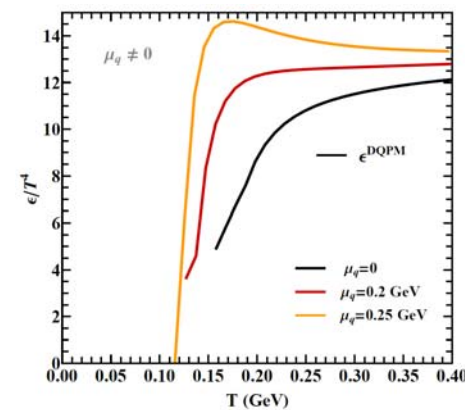
Entropy density at finite (T, μ_q)



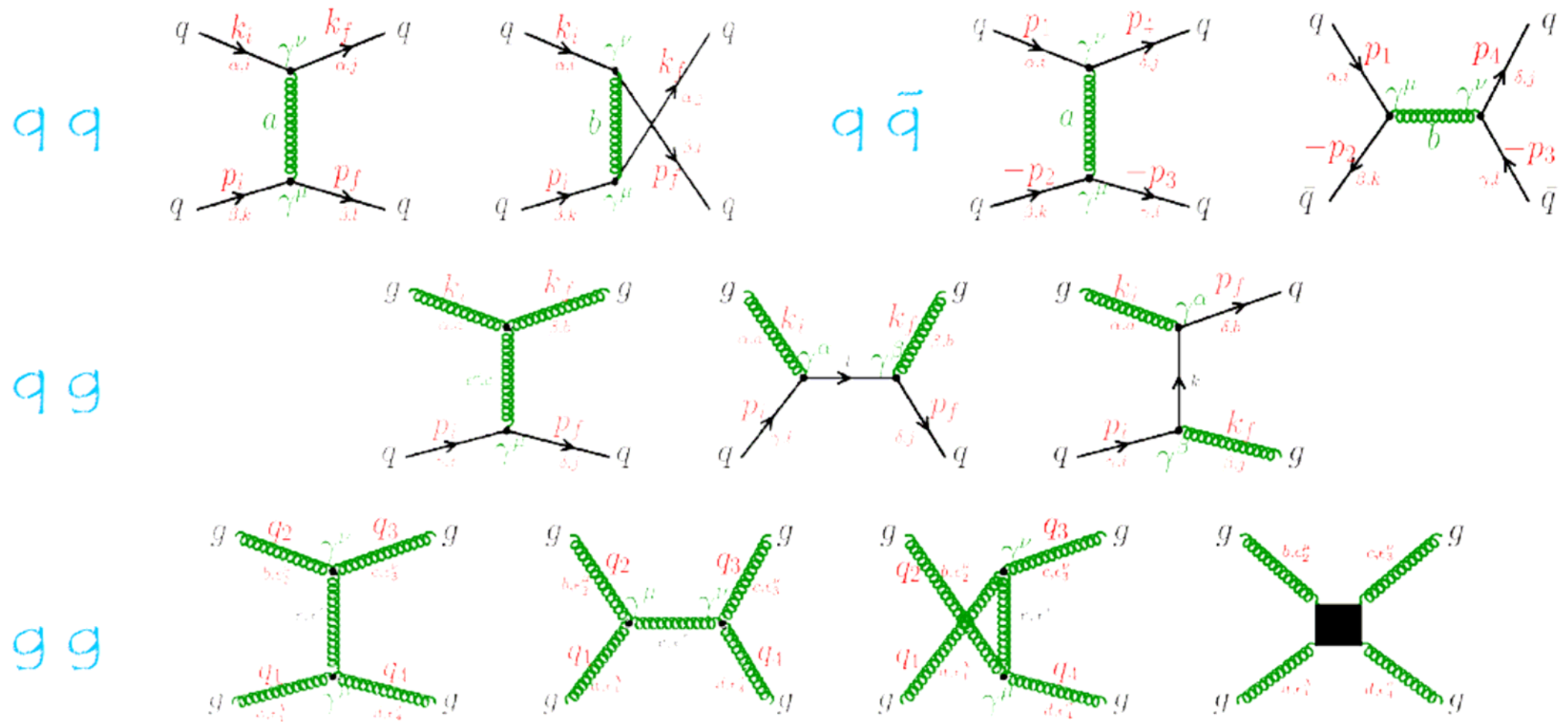
□ Energy density at finite T



Energy density at finite (T, μ_q)



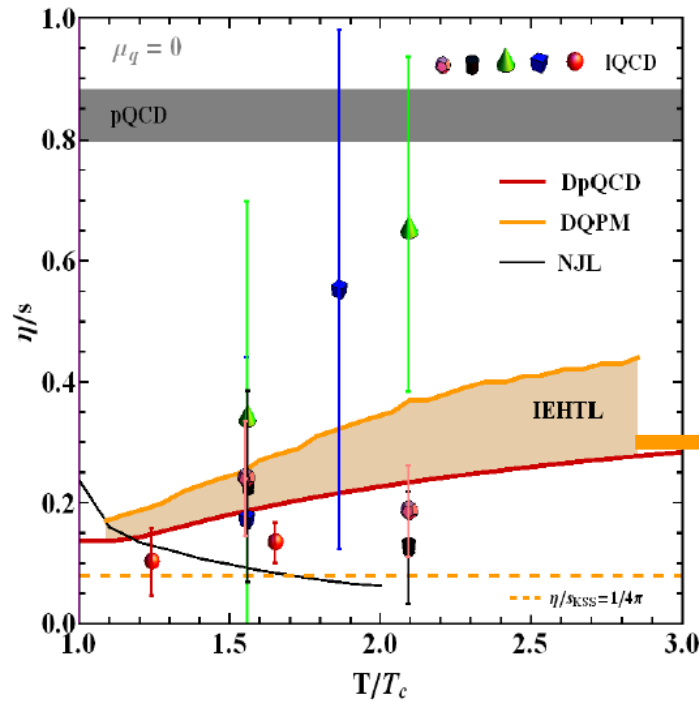
DQPM: q, qbar, g elastic scattering at finite (T , μ_q)



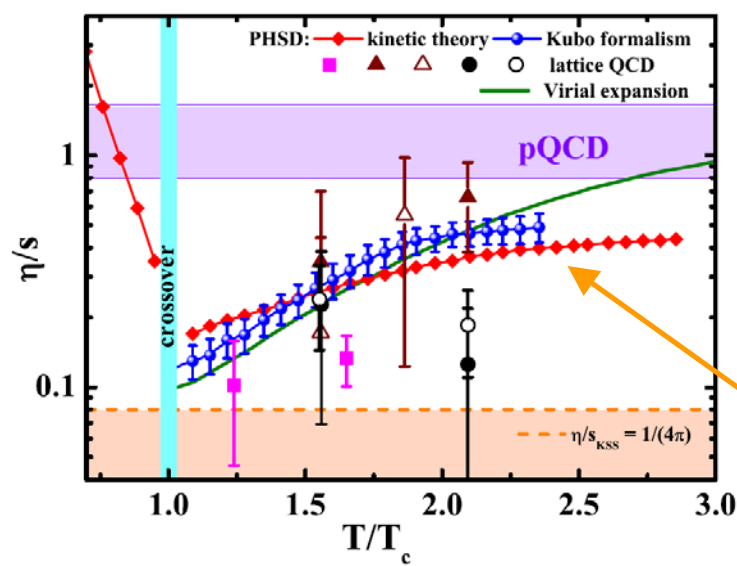
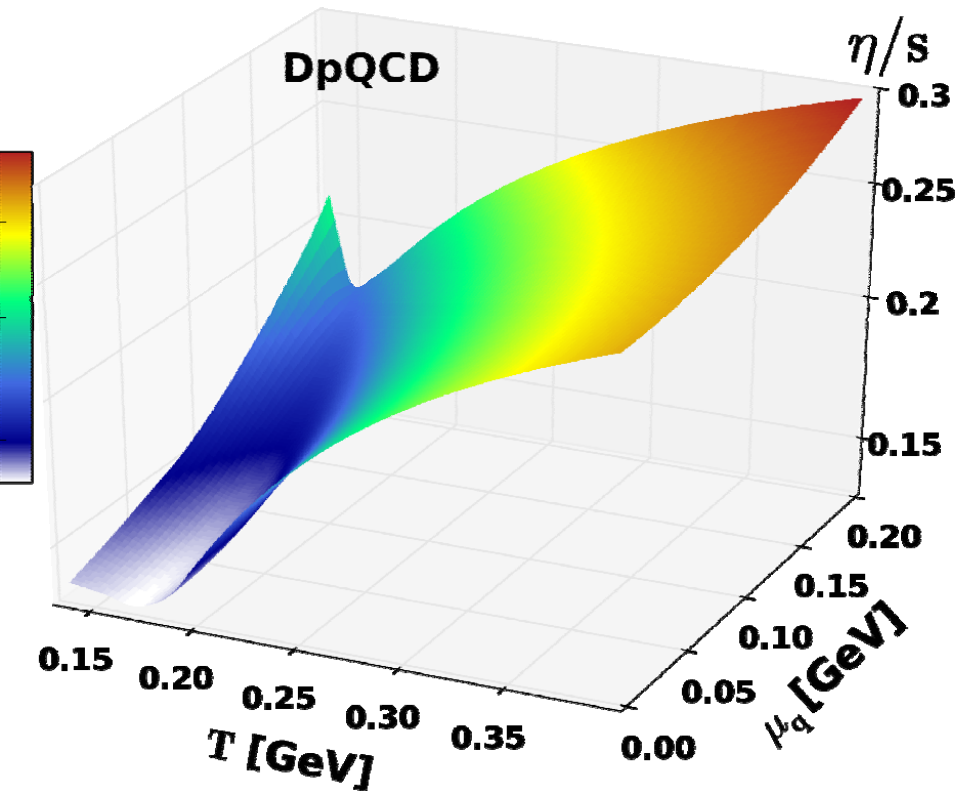
Hamza Berrehrah et al. arXiv:1412.1017

I. DQPM: transport properties at finite (T, μ_q) : η/s

Shear viscosity η/s at finite T



Shear viscosity η/s at finite (T, μ_q)



$\eta/s: \mu_q=0 \rightarrow \text{finite } \mu_q:$
smooth increase as a function of (T, μ_q)

H. Berrehrah et al. arXiv:1412.1017

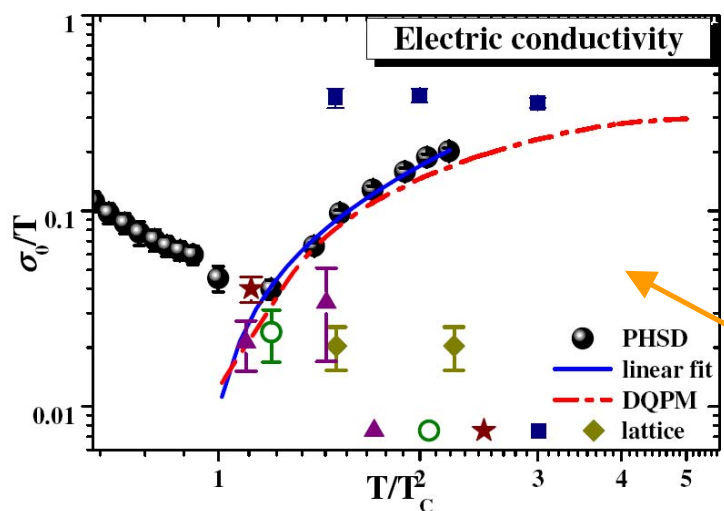
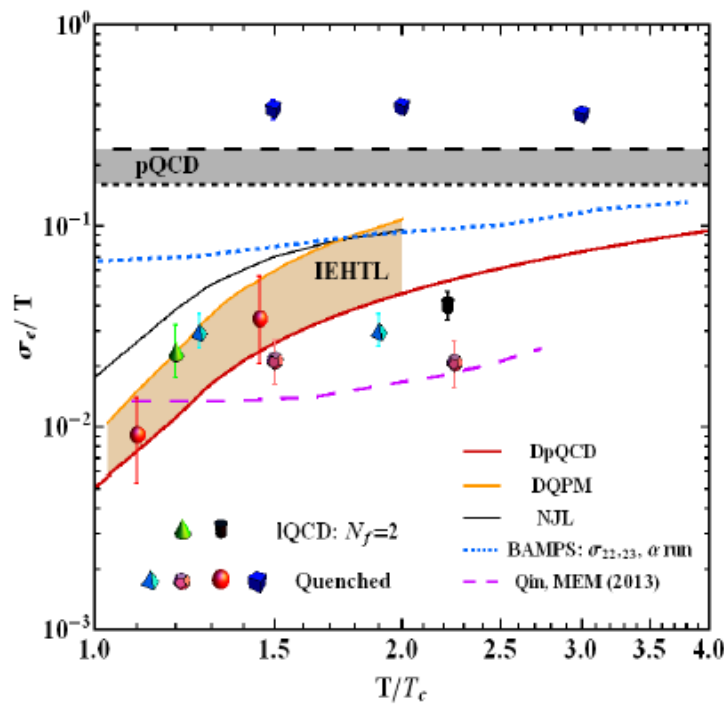
PHSD in a box: V. Ozvenchuk et al., PRC 87 (2013) 064903

Virial expansion: S. Mattiello, W. Cassing, EPJ C70 (2010) 243

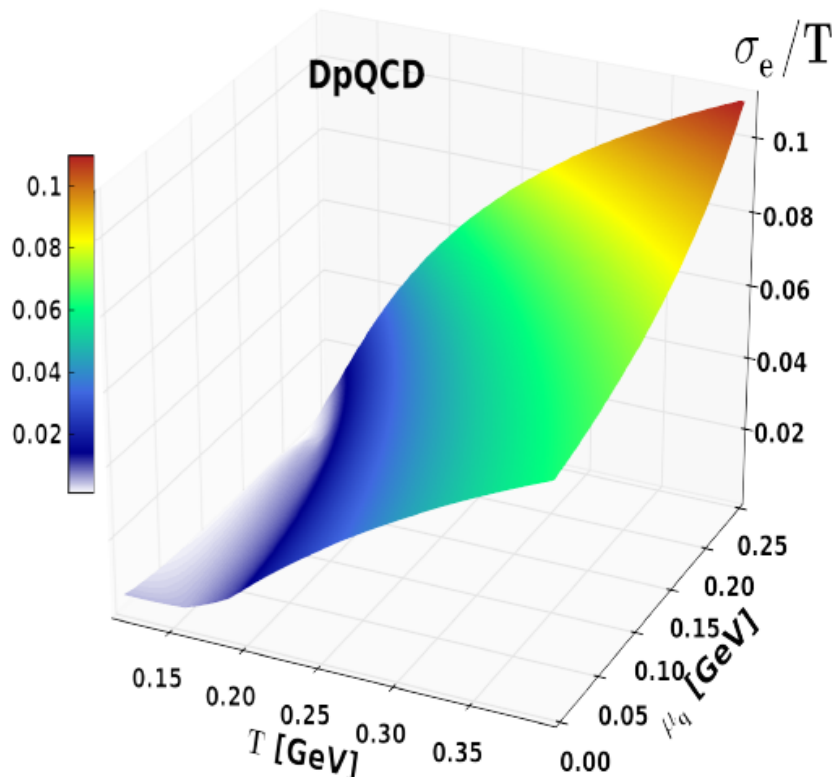
NJL: R. Marty et al., PRC 88 (2013) 045204

II. DQPM: transport properties at finite (T, μ_q) : σ_e/T

Electric conductivity σ_e/T at finite T



Electric conductivity σ_e/T at finite (T, μ_q)



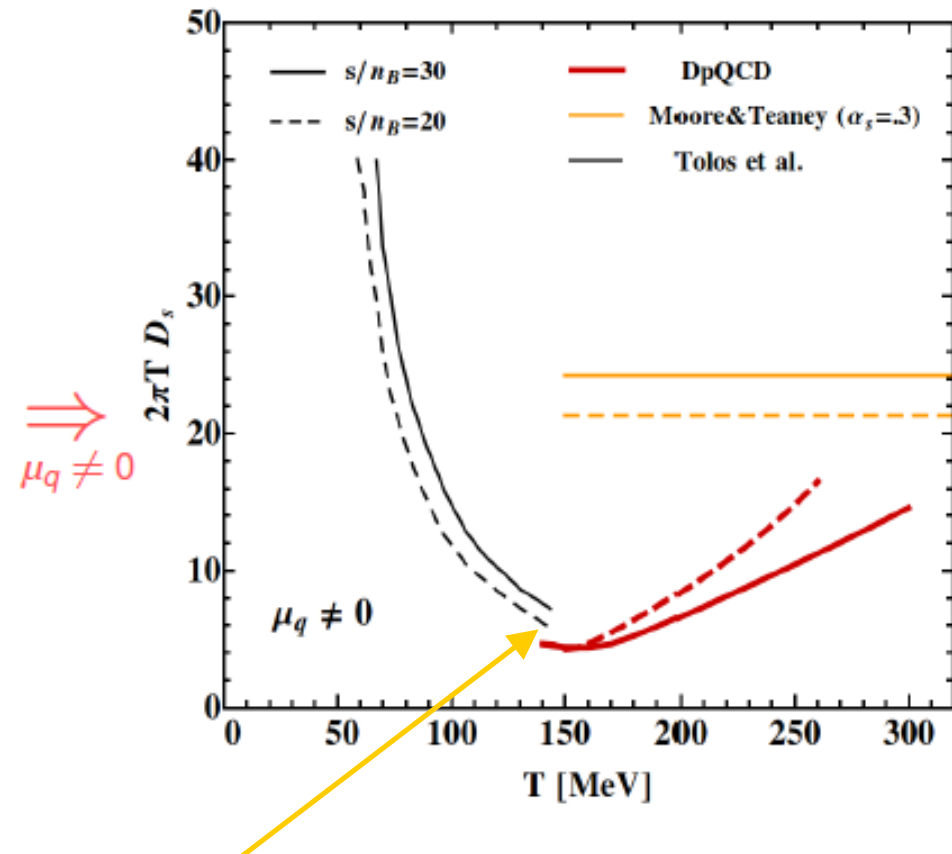
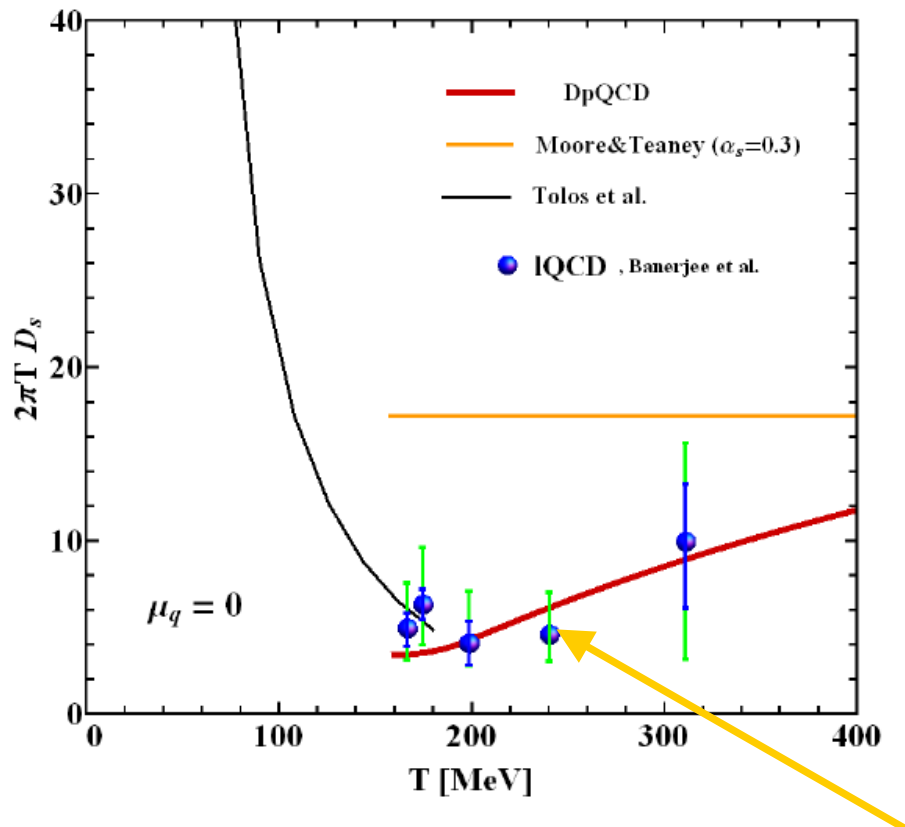
$\sigma_e/T : \mu_q=0 \rightarrow$ finite μ_q :
smooth increase as a function of (T, μ_q)

H. Berrehrah et al. arXiv:1412.1017

PHSD in a box: W. Cassing et al., PRL 110(2013)182301
NJL: R. Marty et al., PRC 88 (2013) 045204

Charm spatial diffusion coefficient D_s in the hot medium

- D_s for heavy quarks as a function of T for $\mu_q=0$ and finite μ_q



□ $T < T_c$: hadronic D_s

L. Tolos , J. M. Torres-Rincon,
Phys. Rev. D 88, 074019 (2013)

→ Continuous transition at T_c !

Summary: DQPM at finite (T, μ_q)

- Extension of the DQPM to finite μ_q using scaling hypothesis for the effective temperature T^*

- $\mu_q=0 \rightarrow$ finite μ_q :
 - variations in the QGP transport coefficients
 - smooth dependence on (T, μ_q)
 - $\eta/s, \zeta/s, \sigma_e/T, D_s$ show minima around T_C at $\mu_q=0$ and finite μ_q

□ Outlook

Implementation into PHSD: from $T, \mu_q=0 \rightarrow$ finite T, μ_q





PHSD group

FIAS & Frankfurt University

Elena Bratkovskaya

Hamza Berrehrah

Daniel Cabrera

Taesoo Song

Andrej Ilner

Rudy Marty (→Lyon Uni.)

Giessen University

Wolfgang Cassing

Olena Linnyk

Volodya Konchakovski

Thorsten Steinert

Alessia Palmese

Eduard Seifert



External Collaborations

SUBATECH, Nantes University:

Jörg Aichelin

Christoph Hartnack

Pol-Bernard Gossiaux

Vitalii Ozvenchuk



Texas A&M University:

Che-Ming Ko

JINR, Dubna:

Viacheslav Toneev

Vadim Voronyuk



BITP, Kiev University:

Mark Gorenstein

Barcelona University:

Laura Tolos

Angel Ramos



Thank you!